Investigation of WDM VLC Using Standard 5 mm RGB LEDs

Andrew Burton, Stanislav Zvanovec, Zabih Ghassemlooy, Paul Anthony Haigh, Izzat Darwazeh, Hoa Le Minh

Investigation of WDM VLC Using Standard 5 mm RGB LEDs

Andrew Burton
OCRG, Faculty of Engineering and Environment
Northumbria university
Newcastle upon Tyne, UK
andrew2.burton@northumbria.ac.uk

Zabih Ghassemlooy
OCRG, Faculty of Engineering and Environment
Northumbria university
Newcastle upon Tyne, UK
z.ghassemlooy@northumbria.ac.uk

Izzat Darwazeh
Department of Electronic and Electrical Engineering
University College London
London, UK
i.darwazeh@ucl.ac.uk

Stanislav Zvanovec
Department of Electromagnetic Field
Czech Technical University in Prague
Prague, CR
xzvanove@fel.cvut.cz

Paul Anthony Haigh
Department of Electronic and Electrical Engineering
University College London
London, UK
p.haigh@ucl.ac.uk

Hoa Le Minh
OCRG, Faculty of Engineering and Environment
Northumbria university
Newcastle upon Tyne, UK
hoa.le-minh@northumbria.ac.uk

***Abstract*—This paper investigates wavelength division multiplexing (WDM) uisng standard off-the shelf commercial 5 mm red, green, blue chip light-emitting diodes for visible light communications (VLC). From the initial observations of the illuminance footprint, it is found that the illumination overlap from each of the three colours is difficult to achieve a white light due to the physical layout of the emitting elements. We experimentally demonstrate that WDM is only achievable with a horizontal misalignment of +/- 0.5 cm or +/- 2 cm of the origin at a transmission span of 10 and 40 cm. Furthermore, with respect to the angular misalignment, WDM is achievable within a cone area of +5º of the origin at 10 cm distance and only along the origin at a distance of 40 cm.**

Keywords—RGB LED, wavelength division multiplexing, visile light communications.

I. INTRODUCTION

As the demand for high-speed wireless data increases, the strain placed upon the traditional radio frequency (RF) infrastructure is becoming increasingly apparent. Cisco reports that global Internet traffic in 2021 will be the equivalent to 127 times the volume of the entire global Internet in 2005 [1]. This is leading to an 'RF spectrum crisis' as the available spectra cannot satisfy demand. However, optical technologies are ready to offload traffic, working in conjunction with RF technologies. For short-range (a few meters) indoor applications i.e. homes, offices, etc., optical wireless communications (OWC) using the visible spectrum (i.e., wavelengths of 380-760 nm) can be employed. This emerging wireless technology can provide the joint advantage, for the first time ever, of simultaneous data communications, indoor localization and illumination.

Visible light communications (VLC) brings together OWC with the existing lighting infrastructure, providing simultaneous data communications and solid-state lighting, and is driven by light-emitting diode (LED) technologies [2]. The traditional gallium nitride LEDs used for lighting are produced by either coating a single blue chip LED with a yellowish phosphor [3], or through the combination of separate red, green and blue (RGB) chip emitters. Clearly, the first option provides the simplest solution as no colour mixing is required, and the LED manufacturer can supply warm-to-cool white shades depending on the red-to-blue content, such as the Philips Luxeon Rebel range [4]. However, the phosphor coatings on the LEDs have a relatively slow temporal response with respect to the blue chip emitter, hence reducing the available bandwidth B_{LED} of the device by an order of magnitude [5]. This remains a major challenge in realising high-speed VLC systems, hence the requirement for the additional equalisation and spectrally efficient modulation schemes. The RGB type LEDs on the other hand, require additional support for the colour mixing, but do not suffer from the phosphor effect on the available B_{LED}. Additional advantages of RGB LEDs include the possibility to independently deploy each of the individual colour constituents for separate data streams to form wavelength division multiplexing (WDM) and to increase bit rate [6].

The deployment of WDM within VLC has been reported in the literature, supporting bit rates up to 4.05 Gb/s over a transmission link span of 1 m [7]. Furthermore, an aggregate data rate of 6.36 Gb/s has been reported over the same distance, employing a multiple-input multiple-output (MIMO) VLC system [8]. There are many more RGB WDM VLC systems and techniques published in prior art [9-13], however, none of these reportes commentate on the colour mixing capabilities of the LEDs to produce white light with respect to spatial link properties. This paper aims to investigate the ability of WDM with an RGB LED for the VLC system. Particular attention has been paid to the illumination pattern provided by each of the emitters and the overlap between the footprints of the different wavelengths. We demonstrate through the use of a standard off-the-shelf 5 mm RGB LED (Kitronic Ltd, common anode [14]), the technical difficulties for combining the three colours and hence achieving true WDM off the link axis.

The rest of this paper is organised as follows; Section II demonstrates the set of original observations and measurements of the optical output to the RGB LED; Section

III describes WDM VLC experiments, Section IV provides discussion of the results, and finally, Section V draws all of the conclusions.

II. RGB LED Initial Observations and Characterisation

A. Initial Observations

It is clear from observation of the RGB LED footprints that colour mixing of the three chips to produce white light is a challenge with respect to spatial distribution (see Fig. 1). The colour rendered to the observer is not constant; it changes based on the observer's relative position to the LED. For instance, an observer to the geometric left of the LED experiences green shades, whereas and observer on the right encounters more blue tones. Fig. 1 demonstrates this effect, where Fig. 1(a) shows the experimental setup whereby the RGB LED illuminates a white surface (standard A4 paper) over a distance *d*. Figs. 1(b)-(e) shows the resultant colour mixing and individual RGB illumination footprints, which are projected onto the surface from the transmitter (Tx) over a given range *d*. It has been found that, each of the RGB footprints increases in size linearly with respect to *d*. What is also interesting to note is that it would appear that each of the axes of the RGB LEDs are not perfectly aligned in parallel but are offset from each other. Hence, the white overlap becomes less and less the further the Tx is placed away from the illuminated surface.

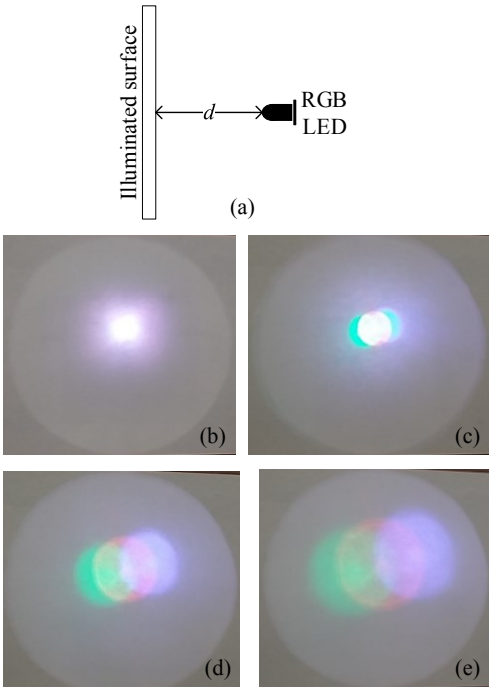

Figure 1(a) experimental setup, (b) illumination footprint at d = 0 cm, (c) d = 5 cm, (d) d = 10 cm, and (e) d = 15 cm

B. LED characterisation

Fig. 2 (a) displays the measured and normalised (to blue) spectral output power for a fixed input drive current I_D of 20 mA applied to each of the coloured chips (note that, the outputs have been normalised to the blue chip). The dotted line denotes the sum of the optical power over all wavelengths. The peak wavelengths, full width half maximum (FWHM) and their normalised peak amplitudes are given in Table 1.

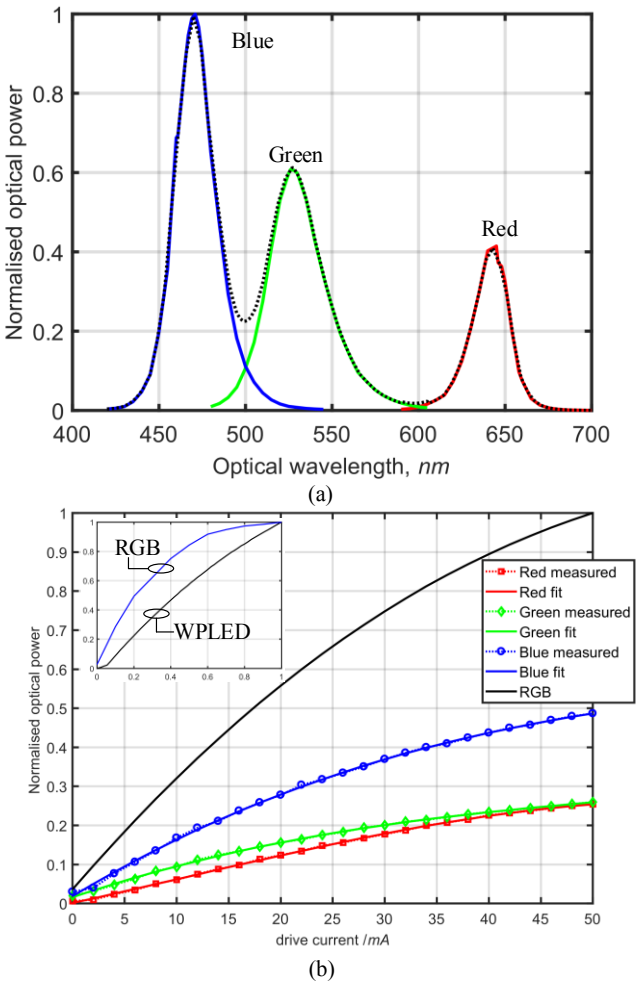

Figure 2 RGB LED: (a) spectral output, and (b) optical output power vs. drive current (inset normalised cd vs. I response of WPLED and RGB LED).

Table 1 Measured spectral outputs of the RGB LED

Colour	Peak spectral output (nm)	FWHM (nm)	Normalised peak amplitude
Red	645	24	0.42
Green	526	35	0.61
Blue	471	30	1.00

Hence, for the same I_D of 20 mA applied to each of the coloured emitters, the blue shows the highest power output with the green showing almost 60% of the blue, and the red at 40%. Likewise, the green shows the widest FWHM followed by the blue and red. In addition, it has been observed that inter colour interference (ICI) occurs between the blue and green emitters. Using the wavelength of 500 nm as a threshold value, 3% of the blue energy is mixing with the green, whereas approximately 3% of the green output is mixing into the blue.

Between the green and red emitters (using a wavelength of 600 nm as a threshold) 0.2% of the green energy is shared into the red, and conversely 0.5% of the total red output is shared with the green. Thus, cross talk between colours is more likely to occur between the blue and green, than the red and green.

Fig. 2 (b) shows the quasi-linear relationship between the input drive current I_D and the normalised output optical power P_W, measured with a power meter (please note that the output power has been normalised to the maximum white RGB output). The fitted curves as a function of I_D are given for the purpose of electro-optic modelling as:

$$P_{\mathrm{Red}}(I_{\mathrm{D}}) = -8.9e^{-7}I_{\mathrm{D}}^3 + 2.8e^{-5}I_{\mathrm{D}}^2 + 5.9e^{-3}I_{\mathrm{D}} + 1.3e^{-3}. \quad (1)$$

$$P_{\mathrm{Green}}(I_{\mathrm{D}}) = 6.4\mathrm{e}^{-7}I_{\mathrm{D}}^3 - 1.2e^{-4}I_{\mathrm{D}}^2 + 9.1e^{-3}I_{\mathrm{D}} + 1.6e^{-2}. \quad (2)$$

$$P_{\mathrm{Blue}}(I_{\mathrm{D}}) = 6.1e^{-7}I_{\mathrm{D}}^3 - 1.6e^{-4}I_{\mathrm{D}}^2 + 1.6e^{-2}I_{\mathrm{D}} + 1.8e^{-2}. \quad (3)$$

$$P_{W\{RGB\}}(I) = P_{\mathrm{Red}}(I) + P_{\mathrm{Green}}(I) + P_{\mathrm{Blue}}(I) \quad (4)$$

$$P_{W\{RGB\}}(I_{\mathrm{D}}) = 3.6e^{-7}I_{\mathrm{D}}^3 - 2.5e^{-4}I_{\mathrm{D}}^2 + 3.1e^{-2}I_{\mathrm{D}} + 3.5e^{-2} \quad (5)$$

For comparison, the inset curves of Fig. 2 (b) show the measured normalised luminous intensity (cd) as a function of the normalised input current I_n for the white response of the RGB LED and a standard white phosphor LED (WPLED). The curves are given by:

$$cd_{WPLED}(I_{\mathrm{n}}) = -1.5e^{-1}I_{\mathrm{n}}^3 - 1.4e^{-1}I_{\mathrm{n}}^2 + 1.3I_{\mathrm{n}} - 3.2e^{-2} \quad (6)$$

$$cd_{RGB}(I_{\mathrm{n}}) = -8.9e^{-1}I_{\mathrm{n}}^3 - 2.7I_{\mathrm{n}}^2 + 2.7I_{\mathrm{n}} - 3.2e^{-2} \quad (7)$$

From the P_W-I response of the LED, the quasi-linear dynamic regions (QLDR) of the emitters have been determined and are given in Table 2. The QLDR is defined where the output optical power is linearly proportional to the input drive current. For binary signalling with two levels (-1 and 1), the QLDR is less important than for multi-level binary signalling; whereby multiple QLDRs will lead to distortion and non-linear variations between signalling levels. Hence, from Table 2 the red emitter has the most linear response with only two QLDRs, and the blue has the least linear with four QLDRs. The total RGB response is given as the sum of the RGB responses, thus with highest appearance to the blue component. The second part of Table 2 compares the luminous intensity as a function of the drive current measured with a Lux metre and compares the RGB and a WPLED. For the white response, the Lux meter had to be used to measure the output as it is not wavelength dependent and the white light is the sum of all visible wavelengths. It must also be noted that both the axis for the inset of Fig. 2(b) have been normalised. The WPLED drive current has been normalised to the maximum WPLED drive current, and the output has been normalised to the maximum WPLED output, likewise the RGB drive current and output have been normalised to the maximum RGB drive current ad output, for ease of visual comparison between the two. Using this method (i.e., using Lux meter), we can see that the WPLED has a higher degree of linearity to the response in comparison to the combined colours of the RGB.

Fig. 3 displays the measured and fitted results of the polar plots for each of the RGB emitters, future work plans to include mmore examples of 5 mm RGB LEDs. Table 3 outlines the fitted half power angle (*HPA*), Lambertian order m and the offset angle. The Lambertian illumination patter is expressed by [15]:

$$I(\emptyset) = I(0)cos^m(\emptyset), \quad (8)$$

where ϕ is the angle of irradiance with respect to the axis normal to the transmitter surface, $I(0)$ is the centre luminous intensity, and m is given by:

$$m = \frac{-\log(2)}{\log(HPA)}. \quad (9)$$

Table 3 Fitted parameters from polar measurements of the LED RGB

Colour	***HPA* (deg)**	**Lambertian order (*m*)**	**Offset angle (deg)**
Red	22	9.2	0
Green	15	20.0	-15
Blue	15	20.0	20

Table 2 QLDR of the emitters

Colour emitter	**QLDR1**		**QLDR2**		**QLDR3**		**QLDR4**	
	I (*mA*)	*P* (*W*)	*I* (*mA*)	*P* (*W*)	*I* (*mA*)	*P* (*W*)	*I* (*mA*)	*P* (*W*)
Red	0-30	0.00-0.18	30-50	0.18-0.25	--	--	--	--
Green	0-14	0.00-0.12	14-40	0.12-0.23	40-50	0.23-0.26	--	--
Blue	0-10	0.00-0.16	10-22	0.16-0.30	22-32	0.30-0.38	32-50	0.38-0.48
RGB	0-12	0.00-0.37	12-24	0.37-0.64	24-36	0.37-0.84	36-50	0.84-1.00
	***I* (*A*)**	***cd***	***I*(*A*)**	***cd***	***I* (*A*)**	***cd***	***I* (*A*)**	***cd***
WPLED	0.05-0.42	0.02-0.48	0.42-0.64	0.48-0.72	0.64-1.00	0.72-1.00	--	--
RGB	0.00-0.20	0.00-0.50	0.20-0.41	0.50-0.76	0.41-0.61	0.76-0.92	0.76-1.00	0.92-1.00

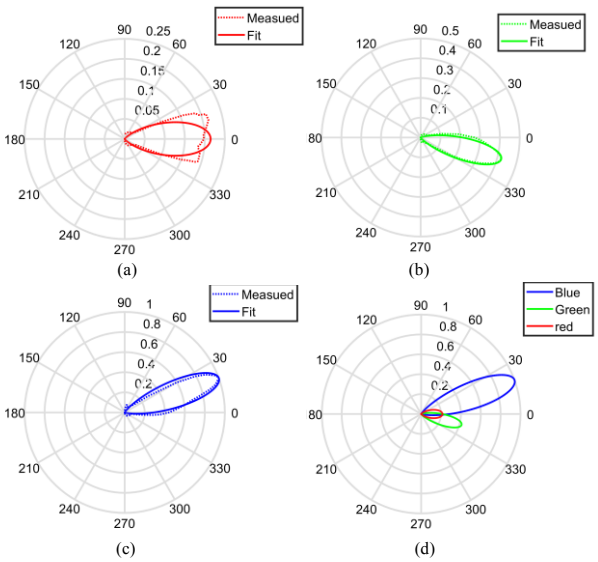

Figure 3 Measured and fit polar plots of the power output at 20 mA input drive current to (a) the red LED, (b) the green, (c) blue, and (d) all three colours.

The polar plots of Fig. 3 have revealed how the emitters have been manufactured onto the 5 mm LED. The red emitter is pointing towards the normal, whereas the blue and green emitters are offset either side of the red. The red chip also provides the smallest Lambertian order m, being approximately half that of the green and blue. The affect of the offset angles on the green and blue emitters will clearly have an effect on the received optical power given by [6]:

$$P_{Rx} = P_{Tx} H(0), \tag{10}$$

where P_{Rx} and P_{Tx} are the received and transmitted power respectively, and $H(0)$ is the DC chanel gain, defined by [6]:

$$H(0) = \begin{cases} \dfrac{(m+1)A}{2\pi d^2} \cos^m(\phi) T_s(\psi) g(\psi) \cos(\psi), & 0 \le \psi \le \Psi_c \\ 0, & \psi > \Psi_c \end{cases} \tag{11}$$

where A is the active area of the PD, d is the distance between the Tx and Rx, ψ and ϕ are the angle of incidence and irradiance respectively, $T_s(\psi)$ is the gain of an optical filter and $g(\psi)$ is the gain of the optical concentrator. The condition Ψ_c signifies the FOV of the Rx. The gain of the optical concentrator is expressed by [6]:

$$g(\psi) = \begin{cases} \dfrac{n^2}{\sin^2 \Psi_c}, & 0 \le \psi \le \Psi_c \\ x, & 0 \ge \Psi_c \end{cases} \tag{12}$$

where n represents the refractive index.

The modulation bandwidth B_{mod} of each of the three colours has also been measured and compared with a standard white phosphor LED. The 3 dB frequency responses outlined in Table 4.

Table 4 also highlights the B_{mod} capabilities of the three emitters with a standard WPLED. As expected, the WPLED has the poorest response due to the slow temporal response of the phosphor coating, whereas the green shows more than double the WPLED and the red and blue having three times greater B_{mod}.

Table 4 Measured RGB and WPLED frequency response

Colour	3dB Frequency response (MHz)
WPLED.	2.7
Red	9.0
Green	7.0
Blue	9.5

III. WDM EXPERIMENTS

A photograph of the WDM VLC experiments is shown in Fig. 4(a). A PC with LabVIEW software automates the control of an arbitrary function generator (AFG3252) and a digital oscilloscope (DSO-X 3034A). The on-off keying non-return to zero (OOK-NRZ) data format is employed for intensity modulating each wavelength at a speed of 10 Mbps, as this falls safely within the B_{mod} capability recorded in Table 4. For the experiments it must be noted that all three emitters were simultaneously illuminated, however only a single colour was modulated per test in order to gain understanding of the optimal performance-per-wavelength without the influence of cross-talk. In each test, a pre-determined data sequence of length 2^{10} was repeatedly transmited through each of the coloured emitters. The received data is captured using a real time digital oscilloscope and stored for offline processing in MATLAB. Each binary bit is determined through midpoint sampling and thresholding of the captured signal, before being compared in a bit-by-bit manner to obtain the system bit error rate (BER) performance. All of the fixed experimental parameters are outlined in Table 5.

Fig. 4(b) shows the experimental configurations for each of the three experiments. The first experiment was carried out to measure the BER as a function of distance d_1 between the LED Tx and the Rx, with and without a lens. All measurements in this test were performed at a transmission/reception angle (ϕ / ψ) of $0^{o,}$ meaning that the receiver position must be adjusted for each wavelength, in order to maintain this condition. The second set of experiments carried out measurement of the BER as a function of the horizontal misalignment between the emitter and Rx (with and without a lens). The Rx is moved along the receiving plane, parallel to the Tx plane. At each test point in distance d_2, the BER is measured. The distance d_1 at $\phi = 0^o$ is kept constant throughout the experiments (10 cm w/o the lens and 40 cm width). The final set of experiments carried out measurement of the BER as a function of the angular misalignment between the Tx and the Rx (once again with and without a lens). For this experiment, the distance d_1 is once again constant (10 cm w/o the lens and 40 cm with), however the Tx's angle ϕ is investigated for the effect on the BER performance.

Table 5 Fixed experimental parameters

Parameter	Value
5 mm RGB LED type	Common anode Kitronik Ltd.
Red, Green, Blue bias current	20 mA
Red, Green, Blue modulation voltage	1.5 Vpk-pk
Modulation format	OOK NRZ
Bit rate, R_B	10 Mbps
Minimum bits to transmit	1e+6
Lens type	Convex
Lens material	Glass
Lens diameter/focal length	25 mm/25 mm
Rx FOV (full angle)	170 deg (w/o lens) 30 deg (w lens)
Rx photodetector (PD)	OSD15-5T
PD active area	15 mm^2
PD rise time	12 ns
PD reverse bias voltage	30 VDC
Rx transimpedance amplifier (TIA)	AD8015
TIA gain	90 Ω
TIA bandwidth	240 MHz

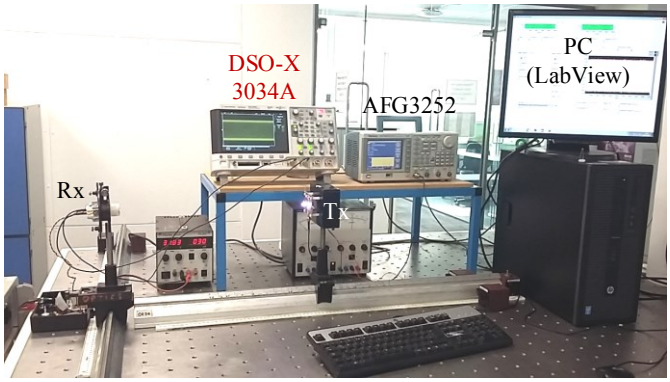

(a)

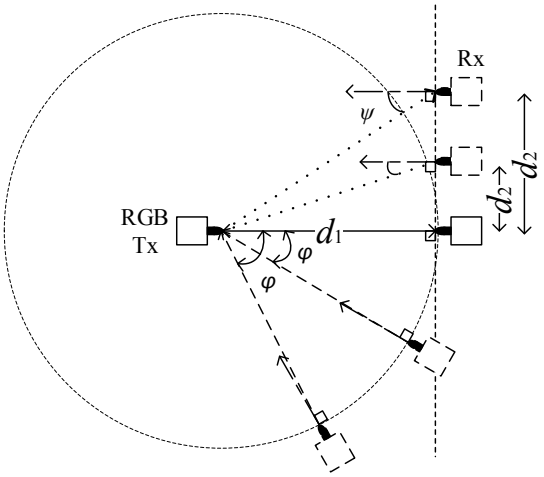

(b)

Figure 4 (a) picture of experimental setup, and (b) experimental configurations.

IV. Results and Discussion

The results of the WDM RGB LED experiments are shown in Fig. 5. Each experiment was performed with and without the lens at the receiver. Figs. 5(a) and (b) show the measured BER as a function of the transmission distance. The results show that the green emitter performs the lowest, as expected due to the fact that it offers the lowest bandwidth. Figs. 5(c)-(f) illustrate the BER as a function of horizontal and angular displacement, respectively. In Figs. 5(c) and (d) the effect of horizontal misalignment has been investigated at a set distance d_1. The distance has been chosen so that each colour maintains a BER of $\leqslant$ 1e-6 at $\psi = 0^o$. Both sets of results display that WDM of the three colours is only possible within a small region of off axis misaligment. Fig. 5(c) shows an overlap where each of the three colours achieve a BER of $\leqslant$ 1e-6 to be only 0.5 cm either side of the origin. Whereas with the addition of a lens (Fig. 5(d)), the WDM region extends to +/- 2 cm either side of the origin. These findings are supported by Eqs. 8 – 11, whereby for the red wavelengths both ψ and ϕ (the angle of incidence and irradiance) are equal, hence the BER being semitrical aout the origin. However, for both the green and blue wavelengths $\psi \neq \phi$ due to the offset shown in Fig. 3, and thus the resultant offset about the origin of their respective BER.

For the angular misalignment, Figs. 5(e) and (f) depict that for a fixed distance, WDM transmission is only possible over a small cone area. Without a lens at a distance of 10 cm, Fig. 5(e) shows that WDM is only achievable within + 5^o of the origin. With the addition of the lens, the WDM communications has been limited to the origin at $\psi = 0^o$. As soon as the Rx moves outside of these limits, potential WDM transmission is no longer possible. Once again we see that this is a result of $\psi \neq \phi$. For the case of the red wavelengths $\psi = \phi$ hence the BER beibng semetrical about the origin, however for the blue and green wavelengths the offset of ϕ is either +/- about the Tx origin. As a result, the Rx and the Tx are no longer aligned and a drop in received optical power is experienced. The drop in the power level reduces the signal to noise ratio and hence increases the BER.

V. Conclusions

This paper has investigated the use of standard 5 mm RGB LEDs for WDM VLC. From initial observations of the luminance footprints, it was noted that, achieving white light from the mixing of the colours was only achievable within a limited region and the observed colour to the user changed with their relative position. Furthermore, measurements of the relative output power per colour with respect to the viewing angle showed that the red emitter faces the normal, however both the green and blue emitters are offset from the normal by -15^o and +20^o respectively. Hence when using the RGB LED for WDM, the physical layout of the emitters makes it very difficult to achieve. Measurements have shown that with no lens, WDM is achievable +/- 0.5 cm of the origin (at a distance of 10 cm) to achieve a BER of <=1e-6; and with a lens (at a distance of 40 cm) the WDM region persists at +/- 2 cm of the

origin. With respect to the transmission/reception angle analysis, it was shown that without a lens (at a distance of 10 cm) WDM is achievable within a +5° cone of the origin; and with the addition of the lens the WDM cone (maintaining a BER of <=1e-6) was severely limited to the origin or 0^0.

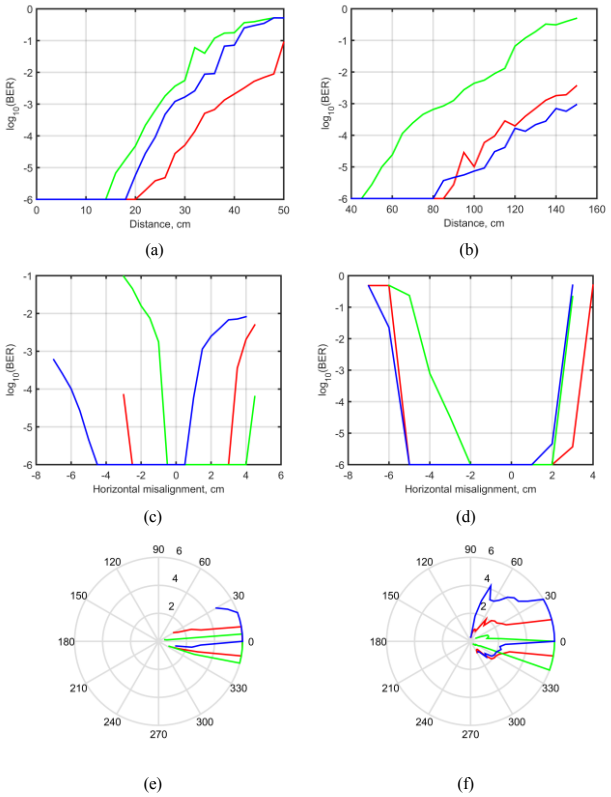

Figure 5 Experimental results of the WDM RGB LED showing: (a) BER as a function of distance between the Tx and Rx w/o lens, (b) with a lens, (c) horizontal displacement w/o lens, (d) with lens, (e) angular misalignment w/o lens, and (f) with lens.

ACKNOWLEDGEMENTS

This work is supported by UK EPSRC Grant EP/P006280/1: Multifunctional Polymer Light-Emitting Diodes with Visible Light Communications (MARVEL), and the EU H2020 Marie Slodowska-Curie grant agreement no 764461 (VISION).

REFERENCES

[1] Cisco. (2017). *Cisco Visual Networking Index: Forecast and Methodology, 2016–2021*. Available: https://www.cisco.com/c/en/us/solutions/collateral/service-provider/visual-networking-index-vni/complete-white-paper-c11-481360.html

[2] S. Rajbhandari, J. J. McKendry, J. Herrnsdorf, H. Chun, G. Faulkner, H. Haas, *et al.*, "A review of gallium nitride LEDs for multi-gigabit-per-second visible light data communications," *Semiconductor Science and Technology,* vol. 32, p. 023001, 2017.

[3] W. O. Popoola, "Impact of VLC on Light Emission Quality of White LEDs," *Journal of Lightwave Technology,* vol. 34, pp. 2526-2532, 2016.

[4] Philips. (2018). *Luxeon rebel series*. Available: https://www.lumileds.com/uploads/28/DS64-pdf

[5] Z. Lubin, M. Hoa Le, D. O. Brien, G. Faulkner, L. Kyungwoo, J. Daekwang, *et al.*, "Equalisation for high-speed Visible Light Communications using white-LEDs," in *2008 6th International Symposium on Communication Systems, Networks and Digital Signal Processing*, 2008, pp. 170-173.

[6] Z. Ghassemlooy, L. N. Alves, S. Zvanovec, and M.-A. Khalighi, *Visible Light Communications: Theory and Applications*: CRC Press, 2017.

[7] M. Zhang, M. Shi, F. Wang, J. Zhao, Y. Zhou, Z. Wang, *et al.*, "4.05-Gb/s RGB LED-based VLC system utilizing PS-Manchester coded Nyquist PAM-8 modulation and hybrid time-frequency domain equalization," in *2017 Optical Fiber Communications Conference and Exhibition (OFC)*, 2017, pp. 1-3.

[8] I. C. Lu, C. H. Lai, C. H. Yeh, and J. Chen, "6.36 Gbit/s RGB LED-based WDM MIMO visible light communication system employing OFDM modulation," in *2017 Optical Fiber Communications Conference and Exhibition (OFC)*, 2017, pp. 1-3.

[9] V. S. R. Krishna and R. Singhal, "720-Mbps 64-QAM-OFDM SCM transmission over RGB-LED-based FSO communication system," in *2016 Thirteenth International Conference on Wireless and Optical Communications Networks (WOCN)*, 2016, pp. 1-5.

[10] Z. Li, C. Zhang, D. Sun, H. Yang, and J. Song, "A real-time high-speed visible light communication system based on RGB-LEDs," in *2017 IEEE International Symposium on Broadband Multimedia Systems and Broadcasting (BMSB)*, 2017, pp. 1-4.

[11] J. M. Luna-Rivera, R. Perez-Jimenez, J. A. Rabadan-Borjes, J. F. Rufo-Torres, V. Guerra, and C. Suarez-Rodriguez, "Multiuser scheme for indoor visible light communications using RGB LEDs," in *3rd IEEE International Work-Conference on Bioinspired Intelligence*, 2014, pp. 119-123.

[12] W. J. Ryu and S. Y. Shin, "RGB MIMO optical camera communication with Histogram equalization," in *2017 International Conference on Signals and Systems (ICSigSys)*, 2017, pp. 303-307.

[13] Y. Wang, R. Li, Y. Wang, and Z. Zhang, "3.25-Gbps visible light communication system based on single carrier frequency domain equalization utilizing an RGB LED," in *OFC 2014*, 2014, pp. 1-3.

[14] (2018). *Kitronik Ltd.* Available: https://www.kitronik.co.uk/3551-rgb-5mm-water-clear-led-45deg-1750mcd-common-anode.html

[15] Z. Ghassemlooy, W. Popoola, and S. Rajbhandari, *Optical wireless communications: system and channel modelling with Matlab®*: CRC press, 2012.